24/09/2020

Minimising embodied carbon in reinforced concrete beams

Amila Jayasinghe

Department of Engineering, University of Cambridge, UK

jaas2@cam.ac.uk

John Orr

Department of Engineering, University of Cambridge, UK

jjo33@cam.ac.uk

Tim Ibell

Department of Architecture & Civil Engineering, University of Bath, UK

abstji@bath.ac.uk

William P Boshoff

Department of Civil Engineering, University of Pretoria, South Africa

billy.boshoff@up.ac.za

Abstract

The construction industry has received attention due to its significant contribution to global carbon emissions. In this paper, conventional design and construction practices of reinforced concrete beams are scrutinised to explore the potential for reductions in embodied carbon. For a given set of design criteria, a family of discrete beam designs which have different geometries and corresponding reinforcements were developed to identify those with minimum embodied carbon. Two algorithms for shape optimisation were developed, one to identify the geometry of the theoretical optimum design, and another considering technical and construction feasibility. Prismatic beams were also optimised exploring alternative designs with different depths and widths along with the required reinforcements, for a reasonable comparison. Several cases were studied to understand the effect of different design parameters. Different design criteria suggested different geometries to minimise embodied carbon, even if the design span was the same. The importance of minimising web width was seen throughout the analysis. The expected deflection of each design was also estimated to understand the effect of optimisation on serviceability performance and found to be satisfactory in all the cases. Embodied carbon of beams can be reduced by up to 38% by optimising prismatic beams compared with conventional designs. Further savings up to 8% are possible with a feasible shape optimised design compared with optimised prismatic beams.

Keywords: parametric design, reinforced concrete beam design, shape optimisation, embodied carbon, deflection

1 Introduction

The built environment accounts for approximately 40% of global energy consumption and 30% of greenhouse gas emissions, according to United Nations Environment Programme [1]. Thus, assessing the environmental performance of buildings is crucial in aiming at sustainability. Ding [2], Ortiz et al. [3], Pomponi and Moncaster [4] and Sharma et al. [5] discussed the methods of measuring the environmental performance of the buildings by analysing different phases of life for their energy consumption and greenhouse gas emissions, while EN 15978 [6] specifies a calculation method. Referring to EN 15978 [6], RICS [7] identifies operational emissions as the result of energy consumption in the day-to-day running of a property whereas embodied emissions as the results from producing, procuring and installing the materials and components of the structure. Since operational carbon is appreciably understood and regulated, Cabeza et al. [8] and Orr et al. [9] suggested that the potential of reducing embodied carbon should be explored equally vigorously in the present context, to reduce whole life carbon emissions of buildings.

Reinforced concrete is widely used in the construction industry. Global production of cement which is mainly used for concrete is around 4.1 gigatonnes [10], being responsible for 5-6% of global carbon emissions [11]. Dimoudi and Tompa [12] and Luo et al. [13] showed that concrete and steel are responsible for 65-75% of total embodied carbon in buildings. Furthermore, Sansom and Pope [14], and Foraboschi et al. [15] identified floor systems were responsible for a share of up to 75% of the overall embodied carbon of the superstructure. Therefore, this paper will explore the possibilities of reducing the embodied carbon of reinforced concrete floor beams.

Prismatic structural members with a uniform longitudinal and transverse reinforcement have the same flexural and shear capacity throughout the member. Such sections are underutilised in several places, implying the potential of reducing material consumption. Shape optimisation is a proven strategy to reduce material usage by providing the necessary amount of material in the right places. Hawkins et al. [16] showed that shape optimisation using flexible formwork can reduce concrete consumption of beams up to 44%. Thus, this study utilises the concept of shape optimisation to minimise embodied carbon of concrete beams.

For a given set of design criteria for a building, there exists a range of viable and safe structural designs that have different grids, element sizes, steel reinforcement design, and even geometries. From the perspective of optimisation, such alternative designs can be analysed to seek the design with minimum possible embodied carbon. For example, if a steel-reinforced concrete beam of a specified span is to be designed to withstand a specified load envelope, there are multiple arrangements of concrete and steel that will satisfy the requirements. Existing design guidelines such as IStructE Design Manual [17] and Concrete Buildings Scheme Design Manual [18] offer span to depth ratios as the starting point for the design process. This paper examines how parametric design could be used to update these starting points to support reductions in embodied carbon in new designs.

According to Orr et al. [19], the depth profiles of the shape optimised beams can be developed considering the flexural performance, and the width profile can be developed considering shear performance. Some adjustments to the depth profile might be required to incorporate shear capacity. However, there might exist more optimal shapes by trading off the width and depth near the ends of the beams in terms of environmental performance. Thus, shape optimisation was considered as a parametric exploration in this study to understand whether the embodied carbon could be further reduced. Therefore, this paper explores the possibility to reduce the embodied carbon of reinforced concrete floor beams through parametric design exploration coupled with shape optimisation.

2 Literature review

Considering the different phases of the lifecycle of building materials, Embodied Carbon of buildings can be reduced by adopting low carbon materials, material minimisation strategies, construction optimisation strategies, local sourcing of materials, material reuse and recycling strategies as shown by Akbarnezhad and Xiao [20], Lupíšek et al. [21], Birgisdottir et al. [22], and International Energy Agency [23]. This study focuses on material minimisation through developing design alternatives. Miller et al. [24], Zeitz et al. [25], Nadoushani and Akbarnezhad [26], Foraboschi et al. [15], and Sahab et al. [27] have successfully illustrated the potential of reducing embodied carbon of buildings by developing design alternatives varying structural form of the building, floor system, reinforcing technique and layout. Going to the next step of optimisation, this study focuses on the reduction in embodied carbon of structural elements by minimising resource usage through understanding the potential trade-off between the choice of the amount of concrete and the reinforcement.

Different researchers have attempted to explore the possibility to reduce the embodied carbon of structural members through developing a range of design solutions. Due to the similarity of the principles, attempts to optimise either cost or embodied energy are also considered in this review. Camp et al. [28], Lee and Ahn [29], and Leps and Sejnoha [30] used genetic algorithms to optimise steel-reinforced concrete frames or beams by varying reinforcement arrangement and sectional dimensions. With the proven savings of around 25-36%, their studies confirm that understanding the trade-off between sectional dimensions and reinforcement may be a promising approach to optimise embodied carbon of concrete members. Kwan et al. [31] optimised two-way span slabs for different span lengths by varying the slab thickness, the grade of concrete, and the amount and strength of reinforcement using genetic algorithms. They observed that the designs with optimum carbon had less concrete and more low strength steel than a conventional design, but the optimum designs were dominated by limiting slab thickness. This further certifies the importance of understanding the trade-off between the amount of steel and concrete chosen in a design. Perea et al. [32] optimised reinforced concrete bridge frames through heuristic optimisation and observed that the optimum designs are governed by the serviceability criteria. Therefore, it is required to assess the serviceability of each discrete design in this study in the optimisation process. Yeo and Gabbai [33] parametrically varied the geometry of and amount of reinforcement in beams to identify optimum and observed a parabolic relationship between depth and embodied carbon, supporting the viability of parametric design approach for optimisation. The above studies adhered to selected existing design codes for the design limitations even if they designed the structural elements with varying dimensions and reinforcement configurations.

Several researchers have reduced the concrete consumption of beams using different design and construction techniques. Xie and Steven [34], Huang and Xie [35], Huang et al. [36], Bendose and Kikuchi [37], Jantos et al. [38], and Gaganelis et al. [39] researched algorithms for topology optimisation which can reduce material consumption by changing the geometry and forming voids. Jewett and Carstensen [40] successfully tested a topology optimised beam with a CNC cut Styrofoam mould reducing concrete usage by 50%. Vantyghem et al. [41] 3D printed a topology optimised post-tensioned beam using 20% less concrete. Veenendaal et al.[42], Garbett et al. [43] and Orr et al. [19,44] used flexible fabric formwork to cast shape optimised reinforced concrete beams reducing concrete usage up to 58%, 55% and

40% respectively. Apart from the minimised concrete consumption, Hawkins et al. [16] identified additional benefits of fabric formwork such as improved durability, textured surface finish, and reduced weight of formwork due to permeable fabric formwork. Therefore, this paper studies the shape optimisation of beams, further exploring the design aspect from a parametric point of view.

Though embodied carbon has been used as a popular assessment method for environmental performance, it has some degree of uncertainty. Hammond and Jones [45] suggested that embodied carbon coefficients should be generally considered tentative. Omar et al. [46] and Dixit et al. [47] illustrated that embodied carbon coefficients can be geographically and temporally inconsistent. Furthermore, Oh et al. [48] pointed out that adhering to present databases may not be a solution for sustainable design due to extreme inconsistencies in the present literature. As an example, the average embodied carbon of C 28/35 concrete is 0.126 $kgCO_2e/kg$ as per The Inventory of Carbon and Energy [49]. The value can be increased to 0.136 $kgCO_2e/kg$ when only CEM I is used or decreased to 0.099 $kgCO_2e/kg$ when fly ash is used for 40%. While the world average embodied carbon of steel rebar is 1.99 $kgCO_2e/kg$, using 85% recycled steel will reduce the coefficient to 1.20 $kgCO_2e/kg$. Furthermore, the reports by Energy Transitions Commission [50] and Material Economics [51] highlight the possibilities of decarbonising the steel industry. Therefore, this study illustrates how sensitive the optimum designs are to carbon coefficients as well.

Design codes such as EN 1992-1-1 [52] and ACI 318 [53] require Ultimate Limit State and Serviceability Limit State to be considered in the reinforced concrete design to provide functional structures. Those codes of practice often offer span/depth ratios as the starting points of the design to tackle deflection conservatively. Further, the design codes impose limits to allowable deflection as a predefined fraction of span. Different researchers have questioned those conventions considering both the design approach and the design limit. Stewart [54] developed a probabilistic model for deflection of reinforced concrete beams sized according to span/depth ratios and proved that the probabilities of serviceability failures are not consistent. Vollum and Hossain [55] conducted a series of parametric studies and concluded that there is scope to reduce slab thicknesses below some conventional guidelines. Further, Orr et al. [56] presented findings of a survey of the structural engineering design profession which showed that 47% of respondents were comfortable in allowing the deflection to exceed the design deflection limit for a few minutes per week or more, even if the limiting deflection of beams and slabs are prescribed by different design guidelines. Therefore, it is rational to estimate the deflections with structural mechanics-based calculations in this study for each design and evaluate how the optimisation process can affect serviceability.

3 Objective

In this study, the approach for the design and construction of concrete beams passively reinforced with steel is revisited to reduce embodied carbon. Exhaustive parametric design together with shape optimisation is used to explore the design space against the conventional design of prismatic beams. Parametric design in this context refers to the design of a set of beams which have different shapes and corresponding amounts of reinforcement in longitudinal and transverse directions to comply with a specified set of design criteria. The intention is to identify the combination of beam geometry and the amount of reinforcement which provides enough capacity with the lowest embodied carbon. Optimisation algorithms are developed to obtain the designs with theoretical optimum and feasible optimum. Prismatic beams are also optimised to facilitate a fair understanding of the benefit of shape optimisation. Since conventional span/depth ratios are not considered as the starting point of the design process, the deflection of each design is estimated and compared against prescribed benchmarks.

4 Methodology

To illustrate the effect of the parametric design approach and shape optimisation, a set of shape optimised beams and a set of prismatic beams were designed to withstand a specified structural requirement. Embodied carbon of all the designs was calculated to identify the design with the minimum environmental impact. Deflections of each design were also estimated. For the sake of simplicity, simply supported reinforced concrete single-spanning flanged floor beams with loadings corresponding to a general office building were analysed in this study. Due to the repetitive nature of the parametric design calculations, MATLAB programmes were developed for designing the beams.

4.1 Design Criteria

One-way-spanning T-beams between columns, which support a two-way-spanning slab around its edges were studied in this paper. The beams were designed considering flexural and shear performance while the resulting designs were assessed for deflection. The following design criteria were considered for both prismatic and shape optimised beams (Figure 1 and Table 1).

- Three sets of design criteria were studied, namely, 8m span simply supported beams in grids of 8m×8m, 8m×6m and 8m×4m, aiming to study the effect on the optimum design from the design load. This selection of the grids captures a range of possible design loads for 8 m span beams within the borderlines of one-way spanning and two-way spanning slabs. Furthermore, the grid choices can be justified considering the possibility to provide recommended window to core spacings (6-13.5 m for deep plans) with a comfortable aspect ratio, referring to British Council for Offices [57].

- The loadings and factors of safety were considered for a general office building referring to EN 1992-1-1 [52], EN 1990 [58] and IStructE design manual [17]. The load transferred to the beams as uniformly distributed loads was then assessed.
- The adjacent two-way slabs were designed according to Concrete Buildings Scheme Design Manual [18], resulting in overall flange depths of 200 mm, 160 mm and 120 mm for the grids of 8 m × 8 m, 8 m × 6 m and 8 m × 4 m respectively.
- The effective flange widths were estimated according to EN 1992-1-1 [52]
- To keep a provision of cover, the distance from the outer surface to the centre of the bottom reinforcement was selected as 40 mm for all the cases (The cover according to EN 1992-1-1 [52] was 15 mm for conditions of a general office building. The recommended deviation is 10 mm resulting in the nominal cover being 25 mm. The provision kept for shear links and longitudinal reinforcement is 15 mm).
- The amount of longitudinal and transverse reinforcement was assumed to be a continuous variable - the error of not selecting the amount of reinforcement from discrete sets of available bar sizes gives a difference of less than 3% in all cases.
- C 30/37 concrete (compressive cylinder strength of 30 MPa and elastic modulus of 33 GPa according to EN 1992-1-1 [52]) and steel reinforcement (with a tensile yield strength of 500 MPa and elastic modulus of 200 GPa) were used in all cases.

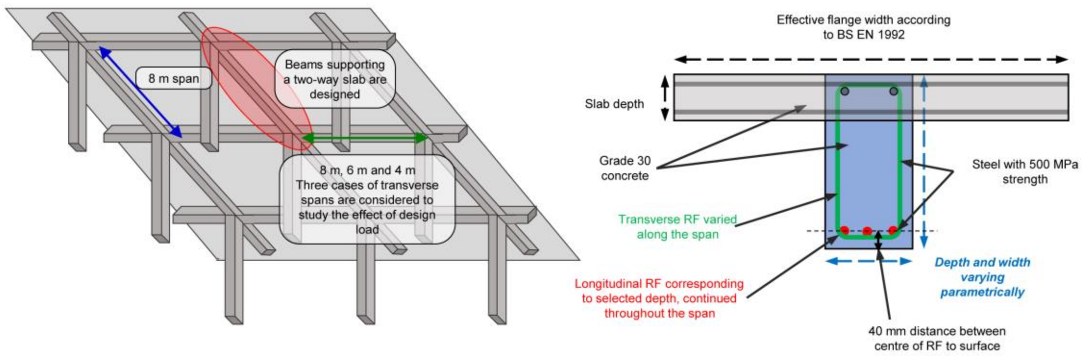

Figure 1. Design criteria of the beams

Table 1. Design details for different load cases

	Load Case 1 (C1)	**Load Case 2 (C2)**	**Load Case 3 (C3)**
Grid Size	8 m x 8 m	8 m x 6 m	8 m x 4 m
Slab depth	200 mm	160 mm	120 mm
Flange width	2240 mm	2240 mm	1860 mm
Self-weight of slab (Gk)	5 kN/m^2	4 kN/m^2	3 kN/m^2
Finishes + Services (Gk)	1.8 + 0.5 kN/m^2	1.8 + 0.5 kN/m^2	1.8 + 0.5 kN/m^2
Partitions + Imposed (Qk)	1.0 + 2.5 kN/m^2	1.0 + 2.5 kN/m^2	1.0 + 2.5 kN/m^2
Load transfer coefficient from slabs to beam (n for $v_{sx}=\beta_{vx}.n.l_x$ according to [18])	0.33	0.41	0.5
Design load for ULS (1.35Gk + 1.5Qk)	79.75 kN/m	67.67 kN/m	49.62 kN/m

Design Load for SLS (Quasi-permanent for deflection - Gk + 0.3Qk)	44.09 kN/m	36.16 kN/m	25.40 kN/m

The longitudinal reinforcement for a selected depth was designed to satisfy the Ultimate Limit State flexural criterion, following EN 1992-1-1 [52]. Since the critical location for bending moment in a simply supported beam carrying uniformly distributed load is at mid-span, this is the defining location to calculate the amount of longitudinal reinforcement, and the same amount was continued throughout the span. All the cases are verified to be within the recommended maximum and minimum amounts of reinforcements stated in EN 1992-1-1 [52]. If the required amount of reinforcement exceeds the maximum reinforcement, the selected geometry was considered structurally unfeasible. The same amount of longitudinal reinforcement was given throughout the beam.

Transverse reinforcement was provided to resist shear which was designed using the variable truss analogy, following EN 1992-1-1 [52] and IStructE Design Manual [17]. The reinforcement was calculated for 11 sections throughout the span, to provide only what is required. The required amount was designed to adopt a strut angle of 22^0 to the horizontal wherever feasible. The minimum recommended reinforcement was provided where the design shear links were unnecessary. The designs in which concrete strut failed were considered unfeasible. The contribution from the flange to the shear capacity has not been considered in this study to be conservative according to EN 1992-1-1 [52,59].

Three different optimisation approaches were adopted in this study, namely, Theoretical Optimum Shape Finding (TOSF), Feasible Optimum Shape Finding

(FOSF), and Optimising Prismatic Beams (Figure 2 & 3). In all three cases, series of design solutions were generated for a range of design midspan depths while each design is optimised for embodied carbon as much as possible through three different approaches. Then the optimum midspan depth for each optimisation approach was identified by plotting the variation of embodied carbon with design midspan depth.

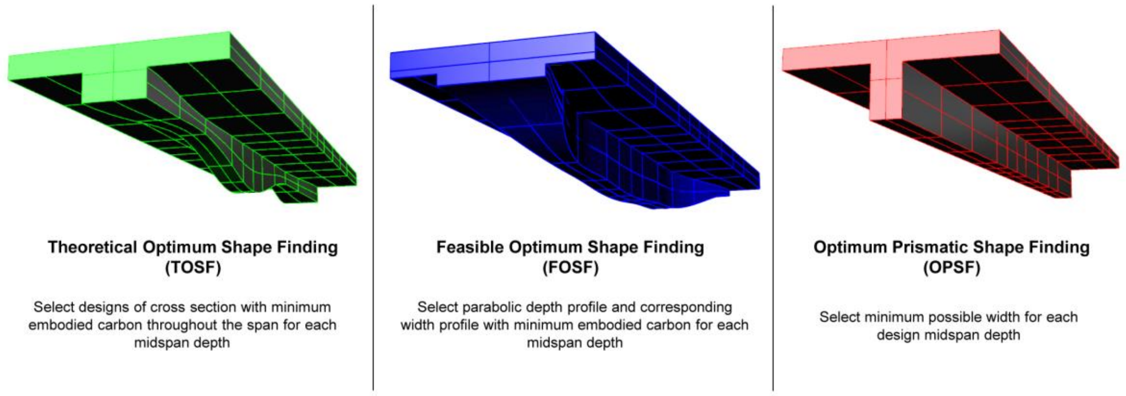

Figure 2. Three different approaches to reduce the embodied carbon of beams

Figure 3. Design flowchart for three different optimisation approaches

4.2 Shape Optimisation

Each generated design solution had a unique depth at midspan, amount of longitudinal reinforcement (which was continued throughout the span), depth profile, width profile and a profile of transverse reinforcement. Though Hawkins et al. [60] mentioned previous work regarding the natural shape of the beam possible using fabric formwork due to fluid concrete pressure, such effects were not considered in this study, for simplicity. The depth and the web width of the beam have been subjected to optimisation, keeping the shape of the web at a given section as a rectangle. The approach for optimisation was developed based on findings by Orr et al. [19,61–63], but an extended parametric design which explores the optimum overall depth and the corresponding shape has been introduced here. The self-weight of the web of the beam was not considered for the sake of simplicity, acknowledging the insignificance of the self-weight of the web compared to other loads. The minimum possible width of the beam was limited to 150 mm and 200 mm as two separate cases, following the fire rating of R60 and R90 [17]. As per the recommendations from Orr [63], the apparently beneficial effect of inclined bars in resisting shear was not considered in the designs.

The process of optimising the shape was approached in two ways. One was to identify the theoretical shape which results in minimum possible embodied carbon, and the other was to identify the design with minimum possible embodied carbon within the constraints of feasible construction. The motivation was to explore the gap between the theoretical best and the practical best in terms of embodied carbon.

4.2.1 Theoretical Optimum Shape Finding (TOSF)

For a given midspan depth, the shape of the beam with minimum possible embodied carbon was explored by designing several sections along the beam in a parametric design approach. First, the amount of longitudinal reinforcement for the selected midspan depth was calculated. Six sections along the beam from the support to the midspan were designed for a range of depths and widths with the predetermined amount of longitudinal reinforcement, taking the advantage of symmetry in the algorithm. Each selection of cross-sectional dimensions for a given section of the beam was estimated for its flexural capacity with the predetermined longitudinal reinforcement and marked structurally unfeasible if the capacity was less than the applied moment at the section. The amount of transverse reinforcement was estimated for each section. Then, the variation of the embodied carbon at each section with design depth and web width was plotted to identify the dimensions which yield the minimum embodied carbon. The shape of the beam with minimum possible embodied carbon for the selected design midspan depth was obtained combining outcomes of such analyses for several sections throughout the beam (Figure 4).

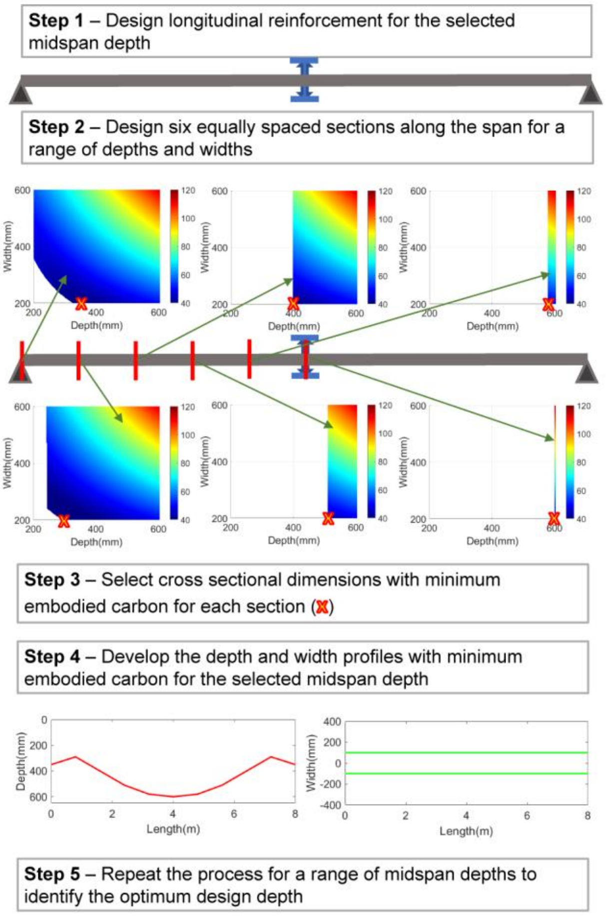

Figure 4. Theoretical Optimum Shape Finding (TOSF)

4.2.2 Feasible Optimum Shape Finding (FOSF)

It is advised to avoid longitudinal reinforcement having both positive and negative curvatures in the design of shape optimised beams since otherwise there will be straightening effects and accompanying vertical forces that add to the shear demand, as shown by Orr et al. [61]. Hence, the design space of shape optimised beams is practically limited to beams with longitudinal reinforcement having a single direction of bar curvature. Therefore, FOSF was focused on finding the configuration of the shape optimised beam with a parabolic depth profile resulting in the minimum possible embodied carbon.

For the selected midspan depth, several parabolic depth profiles were generated by varying the depth at the end of the beam. The corresponding profiles of web width were generated based on shear criteria and minimum width due to fire rating. The reinforcement design is like TOSF. The optimum shape for the selected midspan depth was then selected from the generated pool of designs (Figure 5).

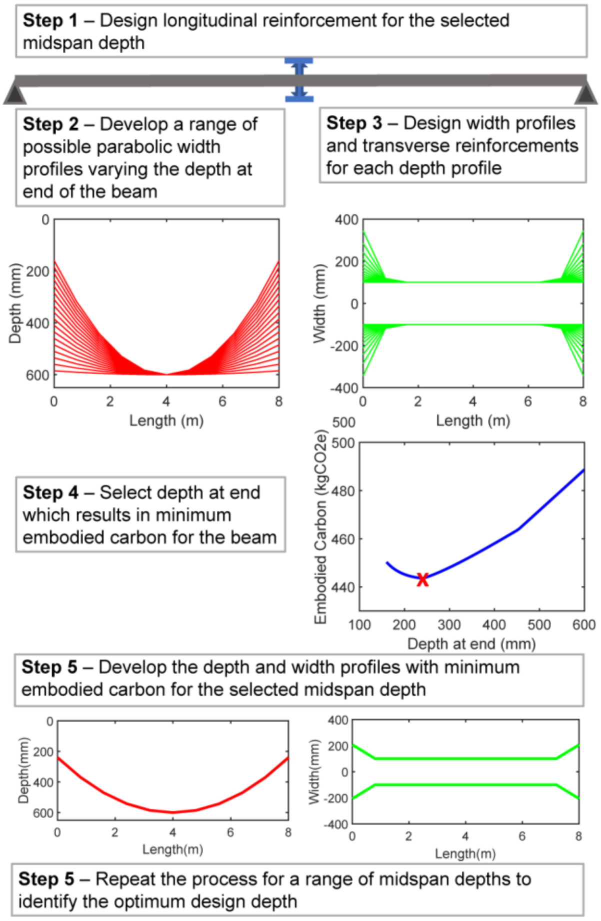

Figure 5. Feasible Optimum Shape Finding (FOSF)

4.3 Optimum Prismatic Shape Finding (OPSF)

For the selected design criteria, sets of discrete beam designs were parametrically developed considering a range of depths which included the conventional design depths (d ≈ span/14). Since the designs are aimed at reducing embodied carbon, width for each design depth was selected as the minimum possible width, which is governed by shear, fire resistance and spacing of reinforcing bars. The minimum width for the shear criterion was calculated to provide a necessary area for a safe concrete strut. Since the fire rating and the space for reinforcement can have an impact on optimum designs, two cases for a minimum width of 150 mm and 200 mm were adopted in this study.

4.4 Estimation of deflection

Deflections of all the beams were estimated by double integration of the curvatures along the beam, following Euler–Bernoulli Beam Theory [64]. Simplified stress blocks for concrete and steel was used to calculate curvatures, referring to EN 1992-1-1 [52]. Concrete was assumed to behave linearly elastic up to the design strength, and then plastic, in compression while tensile strength was neglected. Steel was also assumed to behave linearly elastic up to the design strength in tension. The stress blocks for several sections were developed by numerically solving the relationships for strain compatibility and equilibrium. Then the curvatures along the beam were numerically integrated twice to obtain the deflection profile.

EN 1992-1-1 [52] suggests the calculated sag of a beam under quasi-permanent loads to be less than span/250 for unimpaired appearance and general utility. The quasi-permanent combinations were estimated using ψ_2=0.3 for office areas, following EN 1990 [58]. The effect of creep was considered to account for long-term deflection. Referring to EN 1992-1-1 [52], a creep coefficient equal to 2.0 was chosen to represent the conditions of a general office building, resulting in an effective modulus of elasticity for the concrete of 11 GPa for the quasi-permanent loads. The estimated deflections for the developed designs were compared with the benchmark of span/250 to illustrate how the serviceability requirement might affect the selection of optimum design.

4.5 Estimation of Embodied Carbon

At the end of the analysis, there were prismatic and shape optimised beam designs for three different load cases, designed to satisfy flexure and shear criteria along with the predicted deflections. The Inventory of Carbon and Energy (ICE database) developed at the University of Bath [49] was used to calculate embodied carbon, considering the emissions in the lifecycle phases from A1 to A3 according to EN 15978 [6], i.e. ‘cradle to gate’. Considering the designs to be European in the application, embodied carbon of C30/37 concrete and reinforcing steel were considered as 0.132 $kgCO_2e/kg$ and 1.20 $kgCO_2e/kg$ respectively. In the calculation of embodied carbon, only the web portion of the members was considered (height of the beam × width of the web), because there was no optimisation considered for the slabs in this study. The top reinforcement of the beam and the reinforcement in the flange were also not included for the same reason. The optimisation of slabs will be looked at in future work.

The optimisation algorithms adopted in this study are based on finding an optimum design with minimum embodied carbon by trading off the amounts of steel and concrete. Therefore, the resulting optimum designs are expected to be correlated with the selected embodied carbon coefficients for steel and concrete. A separate study was carried out to understand the effect of selected carbon coefficients on the optimum design. Two additional cases were analysed by increasing and decreasing the carbon coefficient of steel by 50%. The carbon coefficient of concrete is kept constant since the varying coefficient of steel represents the reverse effect of changing the coefficient of concrete. As an example, the impact on the optimum design by increasing the carbon intensity of steel is similar to decreasing the carbon intensity of concrete since both will suggest the optimum to have less concrete and more steel. The choice of the cases is not to represent specific conditions but to generally investigate the effect of the ratio between carbon coefficients of concrete and steel. Load Case C1 and C3 for limiting the minimum possible width to 200 mm were analysed to observe how the optimum midspan depth varies.

5 Results

5.1 Variation of embodied carbon in the design space

The optimisation algorithms considered in this study use design depth and load as independent parameters and required amounts of reinforcements and optimum geometry as dependant variables. Figure 6 shows the variation of flexural and average shear reinforcements for OPSF for three different load cases.

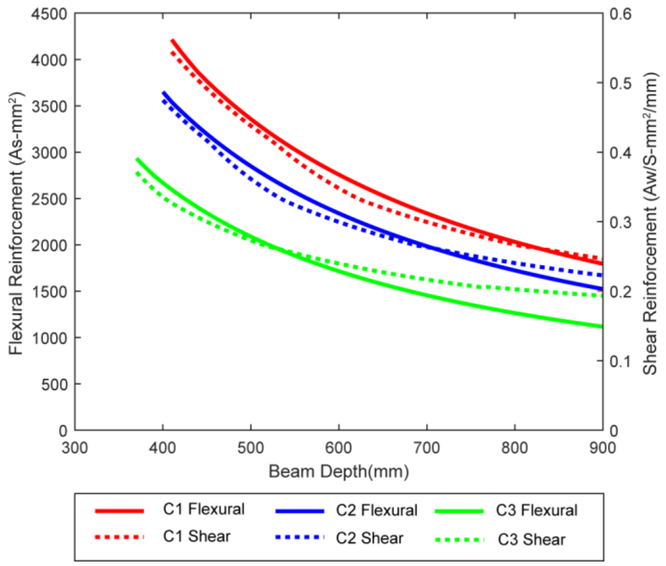

Figure 6. Variation of flexural and shear reinforcement with design beam depth for three load cases for OPSF

Figure 7 presents the variation of embodied carbon with midspan depth for all three optimisation strategies for Load Case C1, breaking down the composition into the contribution from concrete, flexural reinforcement and shear reinforcement. While the amount of flexural reinforcement is unchanged for three optimisation approaches for a given midspan depth, saving of embodied carbon is mainly associated with reducing concrete consumption. The volumes of shear reinforcement were calculated assuming rectangular shear links. Therefore, shape optimisation suggested an increase in the density of shear links while changing the shape of the links. The resulting increase in shear reinforcement has an unnoticeable effect on overall embodied carbon.

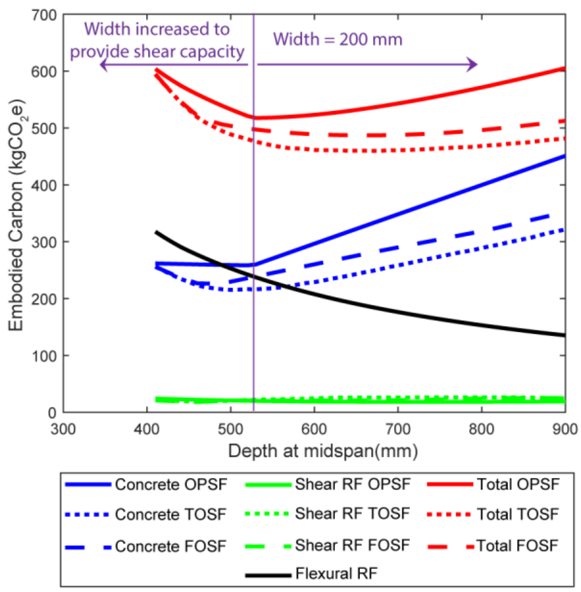

Figure 7. Variation of the composition of embodied carbon with design midspan depth for three optimisation strategies

The curves for embodied carbon from concrete hence the total embodied carbon for OPSF had minimum points with noticeable kinks in the curves. These kinks represent the depths where the criterion for minimum width changes from a shear criterion to fire resistance. The beams shallower than the identified optimum design had widths governed by shear criterion whereas the deeper beams had the selected minimum possible width.

The three different optimisation approaches (TOSF, FOSF and OPSF) were repetitively used to develop discrete designs with different design overall midspan depths for three different load cases (C1, C2 and C3 in Table 1). Further, the beams were designed considering two minimum possible web widths to illustrate the effect on optimum designs. Then, the variation of embodied carbon was plotted to understand the effect of design overall depth, as in Figure 8. As benchmarks, conventional beam designs based on Economic Concrete Frame Elements to Eurocode 2 [65] are also presented in the same plot. Referring to the design charts given in the guide, beam depths for load cases C1, C2 and C3 were selected as 687 mm, 642 mm and 574 mm respectively, for 300 mm wide beams. The interpolated design depths were directly adopted without rounding to approximate the theoretical optimum if the web width was fixed. Minimum points of all the curves which represent the minimum possible embodied carbon for the respective design load for three different optimisation approaches are also marked. Other than the selection of overall beam depth and the web width, the rest of the benchmark designs were performed using the same algorithms used to design prismatic beams.

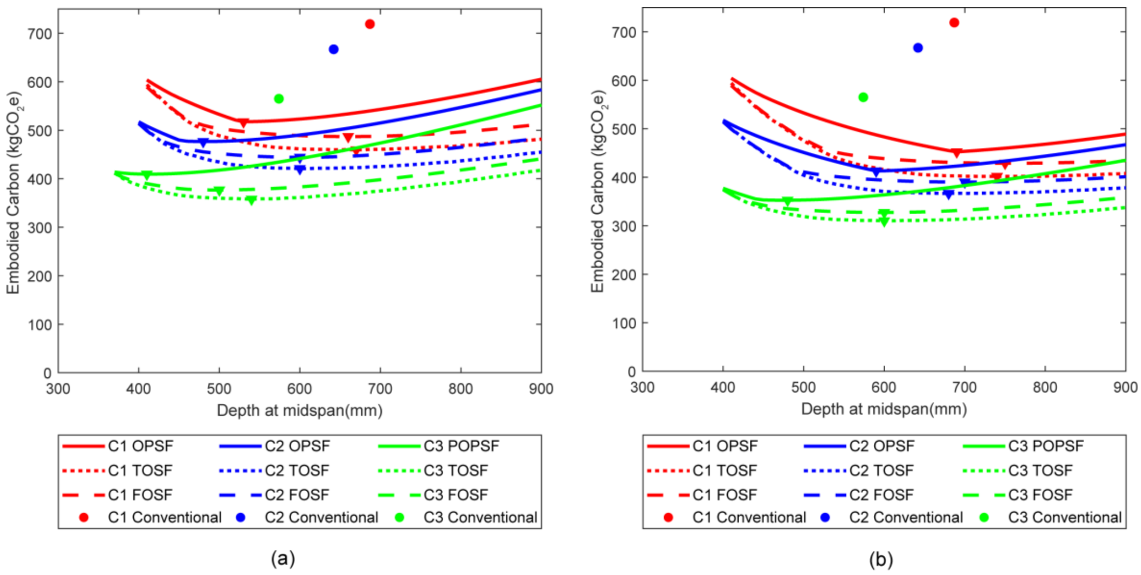

Figure 8. Variation of embodied carbon with design midspan depth for three optimisation approaches when the minimum width of the beams can be (a) 200 mm (b) 150 mm

The curves corresponding to shape optimised beams were generally smooth, but a minimum could be identified. There was a range of midspan depths which exhibited a similar level of embodied carbon around the minimum, indicated by the almost flat regions of the curves. However, the design midspan depths with minimum embodied carbon was notably different for the 18 curves presented in Figure 8, though all the beams had 8 m spans.

5.2 Variation of optimum shape

Figures 9 and 10 demonstrate the identified optimum shapes of the beams from TOSF and FOSF respectively. In both shape optimisation approaches, the optimum geometry varied depending on the design load and the selected minimum possible width. The suggested optimum design midspan depth even varied from 500 mm to 750 mm. In all the cases for TOSF, optimum designs suggested keeping the web width at the minimum possible throughout the beam. At the end of the beam where shear governs the design, the depth profiles were compromised not to increase the web width. In FOSF, the web widths at the ends of the beams were forced to increase so that the depth profile could be parabolic. Since TOSF suggested depth profiles with positive and negative curvatures, FOSF could be treated as the technically feasible approach for shape optimisation.

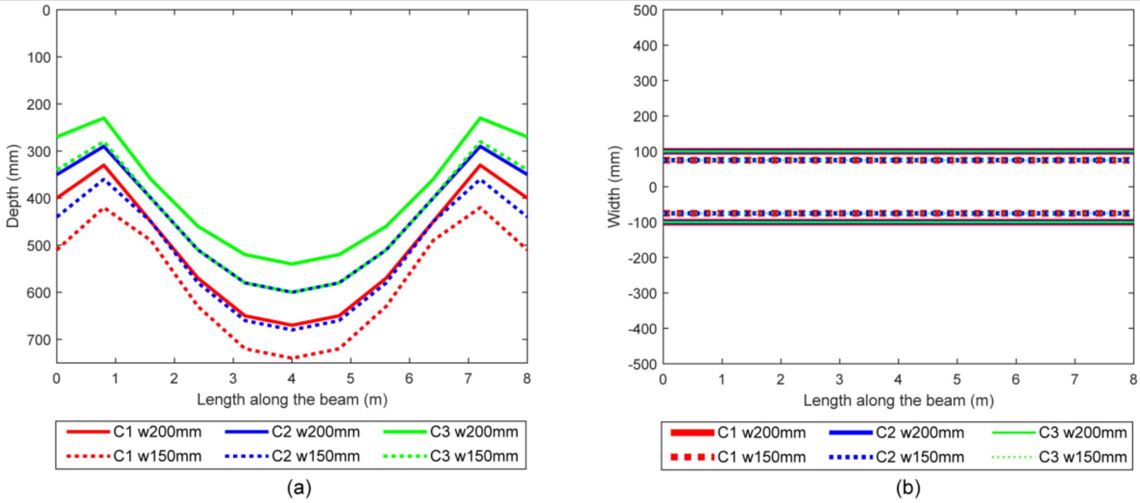

Figure 9. Variation of Optimum (a) Depth Profile (b) Web Width Profile for different design criteria for TOSF

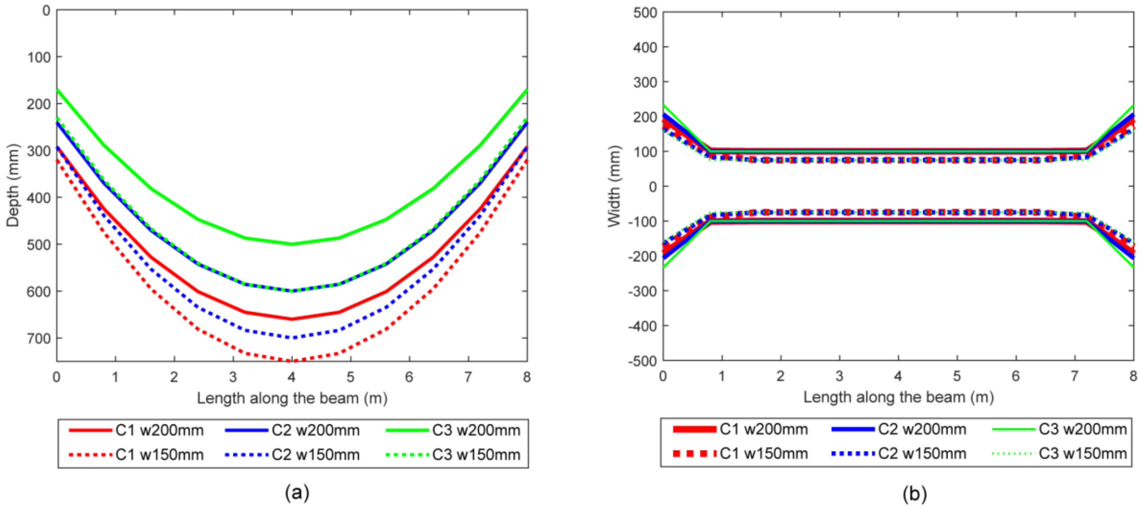

Figure 10. Variation of Optimum (a) Depth Profile (b) Web Width Profile for different design criteria for FOSF

5.3 Deflection performance

Figure 11 presents the variation of estimated deflections for quasi-permanent loads with the design midspan depth for OPSF and FOSF. The figure presents the deflections when the minimum possible width is set to 200 mm rather than 150 mm since the optimisation algorithms suggest shallower beams. The deflections at the optimum designs are also marked. Estimated deflections for conventional design depths were around 40% less than the prescribed limit, highlighting the conservativeness of span/depth ratios for deflection control. Shape optimisation always increased the deflection compared to the prismatic beams. Only the shallow extreme of the studied range of design depths compromised the deflection limit. The designs with minimum embodied carbon from OPSF and FOSF had satisfied the deflection limit for all the design criteria.

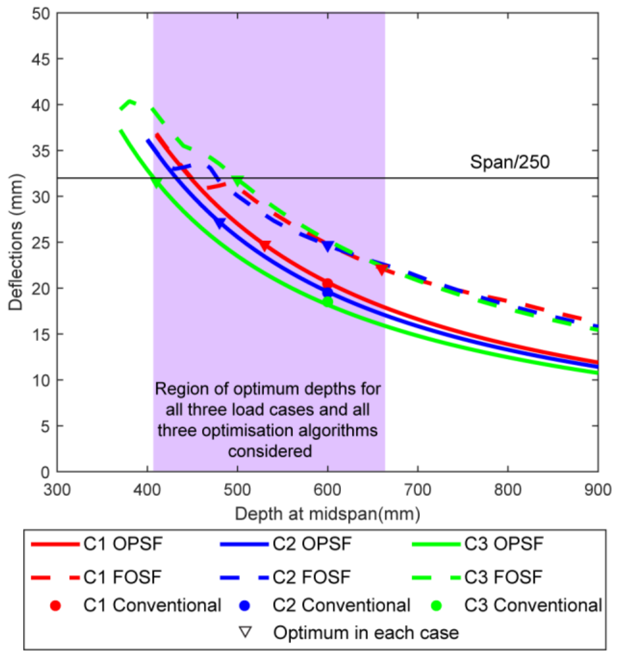

Figure 11. Variation of estimated deflections with design midspan depth for OPSF and FOSF, compared to a conventional benchmark

5.4 Savings of embodied carbon from optimisation

Table 2 presents the savings of embodied carbon from shape optimisation for each design case. The percentage reductions of embodied carbon possible with OPSF, TOSF and FOSF compared to conventional design are noted. Also, the further savings of embodied carbon from TOSF and FOSF compared to OPSF are parallelly reported.

Table 2. Minimum embodied carbon from each optimisation approach compared to conventional designs and savings from each optimisation approach

Design	Embodied Carbon ($kgCO_2e$)				Saving of Embodied Carbon from conventional design (%)			Saving of Embodied Carbon from OPSF (%)	
	Conventional	OPSF	TOSF	FOSF	OPSF	TOSF	FOSF	TOSF	FOSF
Load Case 1/ min width 200 mm	719	518	460	487	28.0	36.0	32.3	11.2	6.0
Load Case 1/ min width 150 mm	719	452	402	429	37.1	44.1	40.3	11.1	5.1
Load Case 2/ min width 200 mm	667	477	421	444	28.5	36.9	33.4	11.7	6.9
Load Case 2/ min width 150 mm	667	413	367	390	38.1	45.0	41.5	11.1	5.6
Load Case 3/ min width 200 mm	565	410	358	377	27.4	36.6	33.3	12.7	8.0
Load Case 3/ min width 150 mm	565	353	310	327	37.5	45.1	42.1	12.2	7.4

To illustrate the differences of the three optimisation approaches adopted in this study, the optimum beam designs suggested for Load Case 1 with a minimum width of 200 mm are presented in Figure 12, along with the possible savings of embodied carbon.

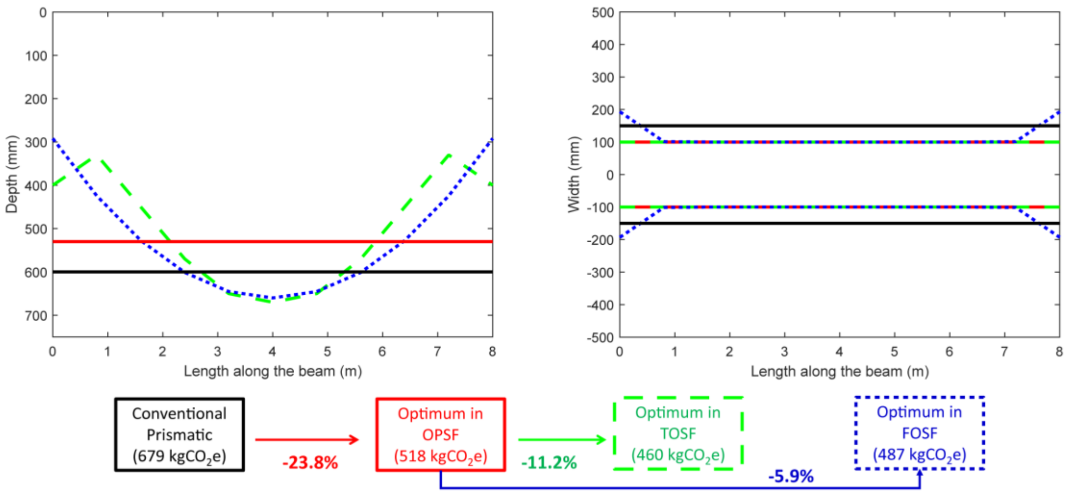

Figure 12. Shapes resulted from different optimisation approaches and possible savings of embodied carbon for the beam with Load Case C1/ minimum width 200 mm

5.5 Influence of carbon coefficients

Figure 13 shows how the optimum design varies for Load Cases C1 and C3 designed with a minimum possible width of 200 mm when the embodied carbon of steel is varied. The optimum design midspan depth of each case is also marked in the same plots. The optimum depth for Load Case C1 varied from 760 mm to 500 mm for FOSF, and from 630 mm to 530 mm for OPSF. The variations were lower for load Case C3. While the optimum depths for OPSF were less sensitive to selected carbon coefficients than FOSF, the curves for OPSF were steeper. It was noticeable that the optimum depth for the OPSF for Load Case C1 remained the same for two scenarios.

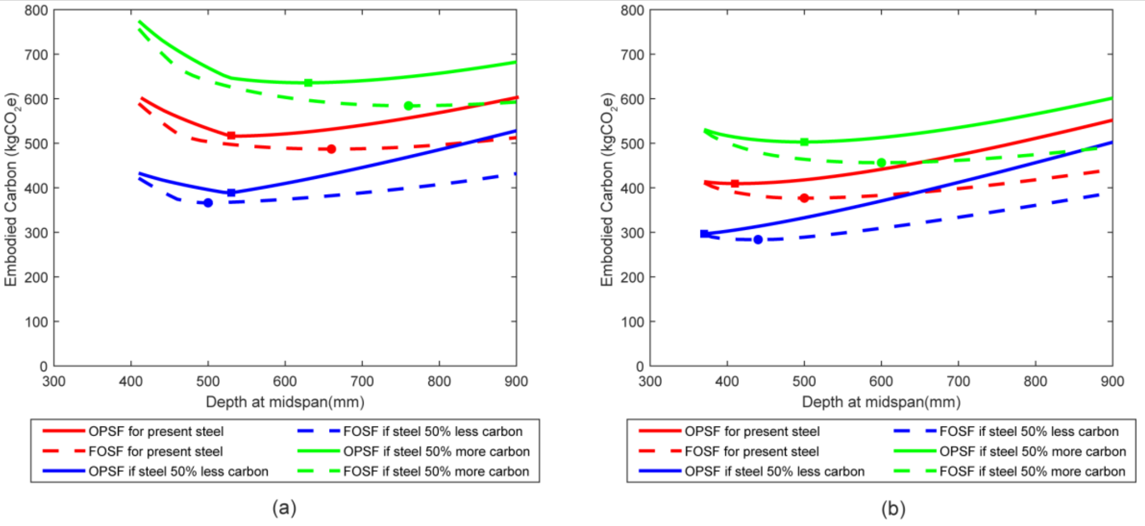

Figure 13. Variation of embodied carbon with design midspan depth (and hence the optimum design midspan depth) for OPSF and FOSF under (a) Load Case C1 (b) Load Case C3 for different carbon coefficients

6 Discussion

6.1 Optimum Shapes

TOSF suggested that the optimum shapes of the beam in all the design scenarios need to keep the web width at the minimum possible web widths for fire criterion or spacing of bars. The depth profiles at the ends of the optimum beams were adjusted to provide an adequate area for the shear performance. The optimisation algorithm selected the deepest cross-sectional design with the area required for the concrete strut so that the amount of shear reinforcement can also be minimised. However, this finding might alter if the shear capacity of the flange was to be accounted for, and this is to be assessed in future work.

The optimum shapes suggested by FOSF had increased web widths at the end of the beams. Still, the depth and web width at the end of the optimum beams varied for different load cases and selected minimum possible widths.

In all the cases for OPSF, the optimum designs were either at the kink of the curve or marginally deeper. Therefore, the optimum prismatic beam designs were significantly affected by the selection of the width of the beam. This highlights the importance of limiting the web width of the beams to reduce embodied carbon.

In all three optimisation approaches, optimum midspan depth and geometry depended on the design load and the selection of a minimum possible width. However, the curves of embodied carbon vs design midspan depths for shape optimisation were smooth with mild slopes, even if the minimum points could be identified. There were ranges of depths at which the shape optimised beam designs had similar embodied carbon.

According to the deflection predictions, prismatic beams with conventional design depths (span/14) have deflection around 60% of the conventional design deflection limit (span/250). Shape optimisation has increased deflection in all cases. However, the predicted deflections of beams with minimum embodied carbon are lower than the conventional design deflection limit in all the cases considered. Hence, the optimisation procedure has not raised concerns about serviceability performance in this study. Therefore, it is worth noting that the optimised designs in all the cases are dominated by Ultimate Limit State. Further, conducting Serviceability Limit State checks with structural mechanics-based calculations help to understand the real extent of design limitations, rather than limiting the design space with conventional span/depth ratios.

6.2 Reduction of embodied carbon

TOSF reduced embodied carbon up to 36% and 45% from conventional prismatic beam designs when the minimum possible widths were 200 mm and 150 mm respectively. Since TOSF resulted in technical and construction challenges, FOSF was adopted which managed to reduce embodied carbon up to 33% and 42% from conventional prismatic beams when minimum widths were limited to 200 mm and 150 mm respectively. However, OPSF could reduce embodied carbon up to 28% and 38% when the minimum possible width is assumed to be 200 mm and 150 mm. TOSF and FOSF could further reduce embodied carbon up to 12% and 8% from OPSF. However, shape optimisation can reduce concrete consumption up to 44% according to the literature review, and the savings of embodied carbon in this study seemed less than the expectation. Therefore, several cases were revisited to assess the reduction of concrete consumption by shape optimisation to evaluate the algorithms in more detail. TOSF and FOSF were observed to reduce concrete consumption up to 30% and 40% respectively for a given midspan depth, though the percentage savings were not consistent across different design criteria. However, optimum midspan depth for prismatic beams and shape optimised beams were not coinciding in almost all the design cases considered in this study. The designs with minimum embodied carbon for prismatic beams and shape optimised beams should be compared with each other to quantify the benefit of shape optimisation, irrespective of the midspan depth. Thus, the percentage reduction of concrete consumption is not directly linked to the saving of embodied carbon from shape optimisation. Due to the need of having positive and negative curvatures in the depth profiles in TOSF, FOSF can be considered as the feasible shape optimisation procedure which could reduce embodied carbon up to 8% compared with OPSF. The interesting outcome is that it seems evident that far greater reductions in carbon footprint are achievable in concrete structures through the prudent analysis of carbon content than by varying the geometry of the structure. The reductions of embodied carbon from all three optimisation algorithms are reduced when the design load is increased, due to the higher need for reinforcement for higher loads.

6.3 Sensitivity of the optimum design to carbon coefficients

The optimisation algorithms find the beam designs with minimum embodied carbon by trading off the volume of concrete and steel. Thus, the dependability of optimum beam designs on adopted carbon coefficients is to be expected. The optimum design depths for FOSF was noticeably varied with the carbon coefficient of steel. That observation can be justified since the designs with minimum embodied carbon would have more steel and less concrete if the carbon intensity of steel reduced. However, the optimum depths of prismatic beams expressed lesser sensitivity to the carbon coefficients. Furthermore, the variation of embodied carbon with midspan depth was steeper in OPSF than FOSF. As the design midspan increases, the increase in the volume of concrete is higher in prismatic beams since shape optimisation could reduce more concrete from a deeper beam. Therefore, variations of carbon coefficients have a lesser effect on optimum prismatic beam designs than shape optimised beam designs. Furthermore, the variation of embodied carbon with midspan depth of OPSF had kinks where minimums were in most of the cases. Therefore, the optimum designs for prismatic beams were less sensitive for changes in carbon coefficients, than shape optimised beams.

6.4 Limitations of the study

The beam geometries suggested by the optimisation algorithms in this study highlighted the importance of minimising the web width of the beams. Though the selected values in this study were associated with fire rating, practically, it may be governed by the spacing of reinforcing bars. Also, the optimisation algorithms suggested different design depths for different cases. Even if the embodied carbon of beams can be reduced through the proposed method, there might be adverse effects on the overall embodied carbon of the building since it may require higher floor to floor heights.

7 Conclusions

The design and construction aspects of concrete beams are scrutinised in this paper to explore the possibilities of minimising embodied carbon. For a given set of structural requirements, a solution with minimum embodied carbon can be identified when the design space is explored. The shape of the beam with minimum possible embodied carbon for a given set of design criteria may have technical and construction objections. Shape optimisation can suggest different geometries for different design criteria, even if the design span is the same. Minimising the web width of the designs is crucial in reducing the embodied carbon of the beams. Such design explorations require deviating from conventional design depths, but the deflection performances of the optimised designs are not compromised. Designs suggested by the shape optimisation algorithms can be very sensitive to adopted carbon coefficients whereas optimising prismatic beams can be less sensitive. Feasible shape optimisation can reduce embodied carbon up to 8% compared with the optimised prismatic beams. However, optimising prismatic beams can save embodied carbon up to 38% compared with conventional design, highlighting the importance of focussing on optimising prismatic beams in practice, and conducting appropriate SLS checks for deflection rather than relying on span-depth ratio checks.

8 Future directions

The influence of the grade of concrete and the shear contribution of the flange on the optimisation requires further study. The possible savings in the two-way spanning floor systems are to be looked at in the next step. However, concrete in passively reinforced flexural members is wasteful since the concrete below the neutral axis is structurally unused. Therefore, techniques to keep concrete mainly in compression such as shell structures and prestressing are also to be looked at parametrically.

9 Data access statement

All data created during this research are openly available from the University of Cambridge data archive at https://doi.org/10.17863/CAM.66855.

10 Acknowledgement

The authors would like to acknowledge the Churchill Jafar Studentship for PhD study at the University of Cambridge.

11 References

[1] UNEP- SBCI. Promoting policies and practices for the build environment. 2019.

[2] Ding GKC. Sustainable construction-The role of environmental assessment tools. J Environ Manage 2008;86:451–64. https://doi.org/10.1016/j.jenvman.2006.12.025.

[3] Ortiz O, Castells F, Sonnemann G. Sustainability in the construction industry : A

review of recent developments based on LCA. Constr Build Mater 2009;23:28–39. https://doi.org/10.1016/j.conbuildmat.2007.11.012.

[4] Pomponi F, Moncaster A. Scrutinising embodied carbon in buildings: The next performance gap made manifest. Renew Sustain Energy Rev 2018;81:2431–42. https://doi.org/10.1016/j.rser.2017.06.049.

[5] Sharma A, Saxena A, Sethi M, Shree V, Varun. Life cycle assessment of buildings: A review. Renew Sustain Energy Rev 2011;15:871–5. https://doi.org/10.1016/j.rser.2010.09.008.

[6] BSI. BS EN 15978:2011: Sustainability of construction works — Assessment of environmental performance of buildings — Calculation method 2011.

[7] RICS. Whole life carbon assessment for the built environment Whole life carbon assessment for the built environment 2017.

[8] Cabeza LF, Barreneche C, Miró L, Martínez M, Fernández AI, Urge-Vorsatz D. Affordable construction towards sustainable buildings: Review on embodied energy in building materials. Curr Opin Environ Sustain 2013;5:229–36. https://doi.org/10.1016/j.cosust.2013.05.005.

[9] Orr J, Drewniok MP, Walker I, Ibell T, Copping A, Emmitt S. Minimising energy in construction : Practitioners' views on material efficiency. Resour Conserv Recycl 2019;140:125–36. https://doi.org/10.1016/j.resconrec.2018.09.015.

[10] U. S. Geological Survey. Mineral Commodity Summaries 2020. 2020. https://doi.org/https://doi.org/10.3133/mcs2020.

[11] UNFCCC. Bigger Climate Action Emerging in Cement Industry | UNFCCC. UN Clim Chang News 2017.

[12] Dimoudi A, Tompa C. Energy and environmental indicators related to construction of office buildings. Resour Conserv Recycl 2008;53:86–95. https://doi.org/10.1016/j.resconrec.2008.09.008.

[13] Luo Z, Yang L, Liu J. Embodied carbon emissions of office building: A case study of China's 78 office buildings. Build Environ 2016;95:365–71. https://doi.org/10.1016/j.buildenv.2015.09.018.

[14] Sansom M, Pope RJ. A comparative embodied carbon assessment of commercial buildings. Struct Eng 2012;90:38–49.

[15] Foraboschi P, Mercanzin M, Trabucco D. Sustainable structural design of tall buildings based on embodied energy. Energy Build 2014;68:254–69. https://doi.org/10.1016/j.enbuild.2013.09.003.

[16] Hawkins WJ, Herrmann M, Ibell TJ, Kromoser B, Michaelski A, Orr JJ, et al. Flexible formwork technologies – a state of the art review. Struct Concr 2016;17:911–35. https://doi.org/10.1002/suco.201600117.

[17] IStructE. Manual for the design of concrete building structures to Eurocode 2. 1.2. London: The Institution of Structural Engineers; 2017.

[18] Brooker O. Concrete Buildings Scheme Design Manual (Eurocode 2 edition). Blackwater: The Concrete Centre; 2009.

[19] Orr J, Darby A, Ibell T, Evernden M. Design methods for flexibly formed concrete beams. Proc ICE - Struct Build 2014;167:654–66. https://doi.org/10.1680/stbu.13.00061.

[20] Akbarnezhad A, Xiao J. Estimation and Minimization of Embodied Carbon of Buildings: A Review. Buildings 2017;7. https://doi.org/10.3390/buildings7010005.

[21] Lupíšek A, Vaculíková M, Št Č, Hodková J, Ĥ R. Design strategies for low embodied carbon and low embodied energy buildings : principles and examples. Energy Procedia 2015;83:147–56. https://doi.org/10.1016/j.egypro.2015.12.205.

[22] Birgisdottir H, Moncaster A, Wiberg AH, Chae C, Yokoyama K, Balouktsi M, et al. Replication Studies paper IEA EBC annex 57 ' evaluation of embodied energy and CO 2eq for building construction .' Energy Build 2017;154:72–80. https://doi.org/10.1016/j.enbuild.2017.08.030.

[23] IEA. IEA EBC ANNEX 57 - Subtask 4: Case studies and recommendations for the reduction of embodied energy and embodied greenhouse gas emissions from buildings. 2016.

[24] Miller D, Doh JH, Mulvey M. Concrete slab comparison and embodied energy optimisation for alternate design and construction techniques. Constr Build Mater 2015;80:329–38. https://doi.org/10.1016/j.conbuildmat.2015.01.071.

[25] Zeitz A, Griffin CT, Dusicka P. Comparing the embodied carbon and energy of a mass timber structure system to typical steel and concrete alternatives for parking garages. Energy Build 2019;199:126–33. https://doi.org/10.1016/j.enbuild.2019.06.047.

[26] Nadoushani ZSM, Akbarnezhad A. Effects of structural system on the life cycle carbon footprint of buildings. Energy Build 2015;102:337–46. https://doi.org/10.1016/j.enbuild.2015.05.044.

[27] Sahab MG, Ashour AF, Toropov V V. Cost optimisation of reinforced concrete flat slab buildings. Eng Struct 2005;27:313–22. https://doi.org/10.1016/j.engstruct.2004.10.002.

[28] Camp C V, Pezeshk S, Hansson H. Flexural Design of Reinforced Concrete Frames Using a Genetic Algorithm. J Struct Eng 2003;129:105–15. https://doi.org/https://doi.org/10.1061/(ASCE)0733-9445(2003)129:1(105).

[29] Lee C, Ahn J. Flexural Design of Reinforced Concrete Frames by Genetic Algorithm. J Struct Eng 2003;129:762–74. https://doi.org/https://doi.org/10.1061/(ASCE)0733-9445(2003)129:6(762).

[30] Leps M, Sejnoha M. New approach to optimization of reinforced concrete beams. Comput Struct 2003;81:1957–66. https://doi.org/10.1016/S0045-7949(03)00215-3.

[31] Kwan B, Glisic B, Ho S, Cho T, Seon H. Comprehensive investigation of embodied carbon emissions , costs , design parameters , and serviceability in optimum green construction of two-way slabs in buildings. J Clean Prod 2019;222:111–28. https://doi.org/10.1016/j.jclepro.2019.03.003.

[32] Perea C, Alcala J, Yepes V, Gonzalez-vidosa F, Hospitaler A. Design of reinforced concrete bridge frames by heuristic optimization. Adv Eng Softw 2008;39:676–88. https://doi.org/10.1016/j.advengsoft.2007.07.007.

[33] Yeo D, Gabbai RD. Sustainable design of reinforced concrete structures through embodied energy optimization. Energy Build 2011;43:2028–33. https://doi.org/10.1016/j.enbuild.2011.04.014.

[34] Xie YM, Steven GP. A simple approach to Structural Optimization. Compurers Struct 1993;49:885–96.

[35] Huang X, Xie YM. A further review of ESO type methods for topology optimization. Struct Multidiscip Optim 2010;41:671–83.

https://doi.org/10.1007/s00158-010-0487-9.

[36] Huang X, Xie YM, Burry MC. A new algorithm for bi-directional evolutionary structural optimization. JSME Int Journal, Ser C Mech Syst Mach Elem Manuf 2007;49:1091–9. https://doi.org/10.1299/jsmec.49.1091.

[37] Martin Philip Bendsoe, Noboru Kikuchi. Generating optimal topologies in structural design using a homogenization method. Comput Methods Appl Mech Eng 1988;71:197–224.

[38] Jantos DR, Riedel C, Hackl K, Junker P. Comparison of thermodynamic topology optimization with SIMP. Contin Mech Thermodyn 2019;31:521–48. https://doi.org/10.1007/s00161-018-0706-y.

[39] Gaganelis G, Jantos DR, Mark P, Junker P. Tension/compression anisotropy enhanced topology design. Struct Multidiscip Optim 2019;59:2227–55. https://doi.org/10.1007/s00158-018-02189-0.

[40] Jewett JL, Carstensen J V. Topology-optimized design, construction and experimental evaluation of concrete beams. Autom Constr 2019;102:59–67. https://doi.org/10.1016/j.autcon.2019.02.001.

[41] Vantyghem G, De Corte W, Shakour E, Amir O. 3D printing of a post-tensioned concrete girder designed by topology optimization. Autom Constr 2020;112:103084. https://doi.org/10.1016/j.autcon.2020.103084.

[42] Veenendaal D, Coenders J, Vambersky J, West M. Design and optimization of fabric-formed beams and trusses: Evolutionary algorithms and form-finding. Struct Concr 2011;12:241–54. https://doi.org/10.1002/suco.201100020.

[43] Garbett J, Darby AP, Ibell TJ. Optimised beam design using innovative fabric-

formed concrete. Adv Struct Eng 2010;13:849–60. https://doi.org/10.1260/1369-4332.13.5.849.

[44] Orr J, Darby AP, Ibell TJ, Evernden MC. Concrete structures using fabric formwork. Struct Eng 2011;89:20–6.

[45] Hammond GP, Jones CI. Embodied energy and carbon in construction materials. Proc Inst Civ Eng - Energy 2008;161:87–98. https://doi.org/10.1680/ener.2008.161.2.87.

[46] Omar WMSW, Doh JH, Panuwatwanich K. Variations in embodied energy and carbon emission intensities of construction materials. Environ Impact Assess Rev 2014;49:31–48. https://doi.org/10.1016/j.eiar.2014.06.003.

[47] Dixit MK, Fernández-Solís JL, Lavy S, Culp CH. Identification of parameters for embodied energy measurement: A literature review. Energy Build 2010;42:1238–47. https://doi.org/10.1016/j.enbuild.2010.02.016.

[48] Oh BK, Choi SW, Park HS. Influence of variations in CO2 emission data upon environmental impact of building construction. J Clean Prod 2017;140:1194–203. https://doi.org/10.1016/j.jclepro.2016.10.041.

[49] Hammond G, Jones C. ICE (Inventory of Carbon & Energy) V3.0 2019.

[50] Energy Transitions Commission. Mission Possible: Reaching net-zero carbon emissions from harder-to-abate sectors by mid-century: Sectoral Focus- Steel. 2019.

[51] Material Economics. The Circular Economy - A powerful force for climate mitigtaion. Stockholm: 2018. https://doi.org/10.1038/531435a.

[52] BSI. BS EN 1992-1-1:2004+A1:2014: Eurocode 2 — Design of concrete structures: Part 1-1: General rules and rules for buildings. 2015.

[53] ACI. ACI 318-14: Building Code Requirements for Structural Concrete and Commentary 2014.

[54] Stewart MG. Serviceability Reliability Analysis of Reinforced Concrete Structures. J Struct Eng 1996;122:794–803.

[55] Vollum RL, Hossain TR. Are existing span-to-depth rules conservative for flat slabs? Mag Concr Res 2002;54:411–21. https://doi.org/10.1680/macr.2002.54.6.411.

[56] Orr JJ, Copping A, Drewniok MP, Emmitt S, Imbell T. Minimising Energy in Construction: Survey of Structural Engineering Practice. 2018.

[57] British Council For Offices. Guideline to Specification. 2019.

[58] BSI. BS EN 1990:2002 +A1:2005- Eurocode - Basis of structural design 2010.

[59] The Concrete Centre. How to Design Concrete Structures using Eurocode 2 Second edition. 2nd ed. London: 2019.

[60] Hawkins W, Orr J, Shepherd P, Ibell T. Fabric formwork : physical modelling for assessment of digital form finding methods. Proc. 11th fib Int. PhD Symp. Civ. Eng., Tokyo: 2016.

[61] Orr J, Darby A, Ibell T, Evernden M. Performance Based Design of Low - Carbon Concrete Structures Using Flexible Formwork. 4th Int Fib Congr 2014 Improv Perform Concr Struct FIB 2014 - Proc 2014:298–9.

[62] Tayfur YR. Optimisation for serviceability of fabric-formed concrete structures.

University of Bath, 2016.

[63] Orr JJ. Flexible formwork for concrete structures. University of Bath, 2012.

[64] Hibbeler RC. Structural Analysis. 8th ed. New Jersey: Pearson Prentice Hall; 2012.

[65] Goodchild CH, Webster RM, Elliott KS. Economic Concrete Frame Elements to Eurocode 2. Concr Cent 2009.